

# Study on the failure behaviour of Advanced High Strength Steel considering stamping history

Ji-chao Zhang<sup>1</sup>, Changwei Lian<sup>1</sup>, and Fei Han<sup>1\*</sup>

<sup>1</sup>Research Institute, Baoshan Iron & Steel Co., Ltd, Shanghai 201900, China.

**Abstract.** The stamping history has a significant impact on the structural performance of ultra-high strength steel parts. In this paper the material hardening and fracture characteristics of QP1180-EL ultra-high strength steel were tested through experimental methods, and the GISSMO damage model parameters were calibrated based on experiment results. A full process simulation analysis was conducted on the stamping process of a bumper beam, and the damage accumulated during the stamping forming process was evaluated based on the GISSMO damage model. The structural performance differences of bumper beam in three-point bending load case were compared and studied under three conditions: without stamping history, with stamping history but except for damage, and with stamping history. The results show that considering thickness reduction, strain, and stress during the forming process can improve the accuracy of predicting structural peak forces, and considering damage during stamping process can further improve the accuracy of predicting structural failure behaviour.

**Keywords:** AHSS; stamping history; GISSMO; QP1180-EL.

## 1 Introduction

Advanced high-strength steel (AHSS) materials are widely used in the body-in-white (BiW) of vehicles in order to meet the increasing requirements of light-weighting and passive safety. Usually, BiW parts need to go through forming processes prior to undergoing deformation in crash tests or real road accident scenarios. To make a precise prediction of vehicle crashworthiness, the forming history of the critical structure parts should be considered during vehicle virtual development stage.

Thickness reduction and work hardening effects of stamping processes on the crashworthiness of front longitudinal beam have been studied [1][2]. A comparative study [3] revealed differences in axial crushing performance of hat-shaped beams among three different forming processes. Research conducted by [4] demonstrated the influence of deep drawing, edge trimming, and spring-back processes on component energy absorption performance. Given the substantial differences between material models in stamping and crash simulations, current crashworthiness evaluations typically incorporate only thickness reduction, plastic strain, and forming-induced stresses while neglecting initial damage caused by plastic deformation during forming stages.

In this paper, the plasticity and fracture behaviour of the 3rd generation AHSS QP-1180EL were characterized using experiment and finite element analysis (FEA) calibration method. Stamping process simulation of an open-profile bumper was carried out and the accumulated damage during the stamping process was evaluated using

a simplified method. The structural performance of the stamped bumper is verified through three-point bending test, and the influence of stamping history on the structural performance of the parts is studied.

## 2 Stamping process damage evaluation

In order to consider the stamping history in the vehicle crash simulation process, finite element analysis software provides mapping capabilities that can transfer history variables from forming simulation to crash simulation. Taking the LS-DYNA solver for example, there are mainly three ways to introduce the accumulated damage during stamping process into crash simulations:

- a) Using LS-DYNA to simulate stamping process, output nodal information, element thickness, strain, stress, and damage history variables from stamping simulation result to the dynain file using the \*INTERFACE\_SPRINGBACK\_LSDYNA keyword, and then directly include them in the crash simulation model using the \*INCLUDE keyword without the need for data mapping. But this method requires the coordinate system, element type, and material constitutive model of the stamping and crash simulation models to be completely consistent, and is only applicable to some simple parts.
- b) Using LS-DYNA to simulate stamping process, output nodal information, element thickness, strain, stress, and damage history variables from stamping simulation result to the dynain file using the \*INTERFACE\_SPRINGBACK\_LSDYNA keyword, and then map the results to the crash model

\* Corresponding author: [hanfei@baosteel.com](mailto:hanfei@baosteel.com)

using the `*INCLUDE_STAMPED_PART` keyword. This method allows for inconsistent coordinate systems, nodes, and mesh types between stamping and crash simulation models, but if damage history variables need to be considered, the constitutive models of stamping and crash simulation materials must be completely consistent.

- c) Using software such as AutoForm/PAM-STAMP for stamping simulation, and then map the simulated results to the LS-DYNA crash simulation model. This method has good flexibility, but cannot map the damage history variables from the stamping process.

Ultra-high strength steel parts are generally thin-walled stamping structures, and during the stamping process, material deformation primarily occurs in a single forming operation. It can be found that during single forming operation, the material deformation process is a quasi-linear strain path. Therefore, based on the element strain, stress state after stamping and GISSMO damage model parameters, the cumulative damage of each element after stamping can be approximately calculated, and introduced to the crash model through `*INITIAL_STRESS_SHELL` keyword history variables. The schematic diagram is shown in Fig. 1.

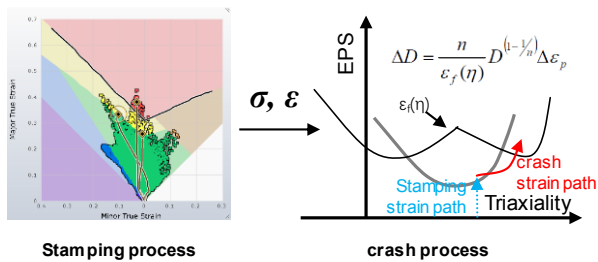


**Fig. 1.** Damage accumulation for stamping process.

Based on the above-mentioned evaluation method, element damage value before spring-back in stamping simulation is calculated as illustrated in Fig. 2. The calculation process and main steps are as follows:

- a) Map the strain and stress tensors from stamping simulation before spring-back to the crash model through `*INITIAL_STRESS_SHELL` keyword;
- b) Calculate the principal stress and stress state at each element integration point;
- c) Calculate the history variables of GISSMO damage model for each integration point based on the stress state, plastic strain and parameters of the material damage model;
- d) Update the damage variables in specified format of the keyword `*INITIAL_STRESS_SHELL` in the crash simulation model.

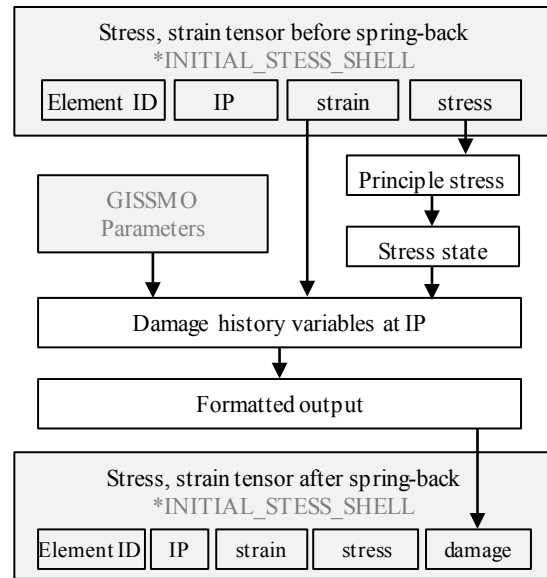


**Fig. 2.** Flowchart for damage accumulation evaluation in stamping process.

### 3 Material characterization of QP steel

QP steel is a typical third-generation advanced high-strength steel. With both high strength and high plasticity, it can meet the needs of automotive users for high-performance ultra-high-strength steel and provide support for the lightweight development of the automotive industry. Table 1 shows the tensile properties of QP1180-EL steel with a thickness of 1.2 mm.

**Table 1.** Tensile properties of QP1180-EL steel.

Steel Grade	Yield Strength (MPa)	Tensile Strength (MPa)	Uniform Elongation (%)	Total Elongation (%)
QP1180-EL	896	1179	11.5	16.3

Based on the uniaxial tensile test data, Swift, Hockett-Sherby, and MPL [5] models were used to fit and extrapolate the stress-strain curve. In-plane torsion and hydraulic bulge test data were used to validate the extrapolation results. All three models provide relatively good fits but show significant differences under large strains, as shown in Fig. 3. In this paper, the MPL hardening model is used in the following simulation.

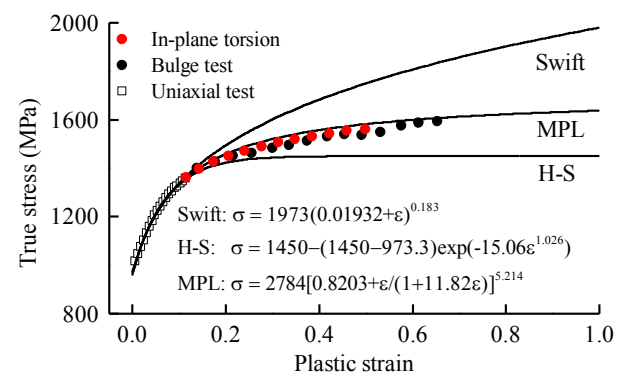


**Fig. 3.** Extrapolation results of different hardening model.

The Generalized Incremental Stress State Dependent Model (GISSMO) developed by Neukamm et al. [6-8] was chosen to describe the failure behavior. In GISSMO model, damage accumulation  $\Delta D$  is calculated at every time step, given by:

$$\Delta D = \frac{DMGEXP}{reg(L_e, \eta) \times \bar{\varepsilon}_f(\eta, \theta)} D^{\left(\frac{DMGEXP-1}{DMGEXP}\right)} \Delta \varepsilon_p \quad (1)$$

where  $\bar{\varepsilon}_f(\eta, \theta)$ ,  $reg(L_e, \eta)$ , and  $DMGEXP$  are the fracture strain, mesh size regularization function and damage accumulation exponent respectively. Modified Mohr-Coulomb (MMC) fracture limit criterion was selected as the fracture strain criterion [9]. The basic formula is as follows:

$$\bar{\varepsilon}_f = \left\{ \frac{A}{c_2} \left[ c_3 + \frac{\sqrt{3}}{2-\sqrt{3}} (1-c_3) \left( \sec \frac{\pi \bar{\theta}}{6} - 1 \right) \right] \right\}^{-\frac{1}{n}} \times \left[ \sqrt{\frac{1+c_1^2}{3}} \cos \frac{\pi \bar{\theta}}{6} + c_1 \left( \eta + \frac{1}{3} \sin \frac{\pi \bar{\theta}}{6} \right) \right] \quad (2)$$

where  $\eta$  is stress triaxiality and  $\bar{\theta}$  is normalized Lode angle,  $A$ ,  $n$  are parameters related to material hardening rule and  $c_1$ ,  $c_2$ ,  $c_3$  are parameters that need to be determined from fracture test.

In order to achieve fracture limit of QP-1180-EL under different stress states and calibrate parameters of MMC fracture model, five different loading cases and testing coupon were selected. These tests covered the stress state of shear, uniaxial tension, stretching, plane strain and equi-biaxial stretching. Schematic of these five individual tests is shown in Fig. 4. The final calibrated MMC model and loading path result of different tests are shown in Fig. 5.

Other undetermined parameters such as damage accumulation exponent, instability limit and fadeout exponent of the GISSMO damage model were calibrated based on the correlation of force-displacement curve

between test and simulation, as shown in Fig. 6. During the calibration process, full integration shell elements with a characteristic length of 1 mm were used for FEA modeling; this ensures the simulation accuracy at the specimen level while improving the regularization accuracy of larger mesh size in subsequent vehicle crash simulations. To better compare the differences between simulation and experimental results, force and displacement data were normalized based on the experimental peak force and fracture displacement respectively. The simulated peak force and displacement at failure are consistent with the experimental results, with an average deviation of less than 5%.

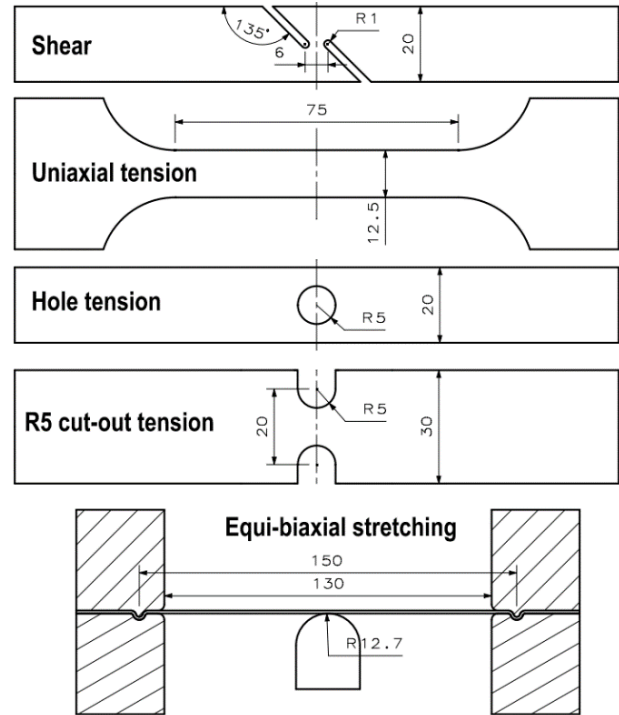


Fig. 4. Fracture limit test specimen.

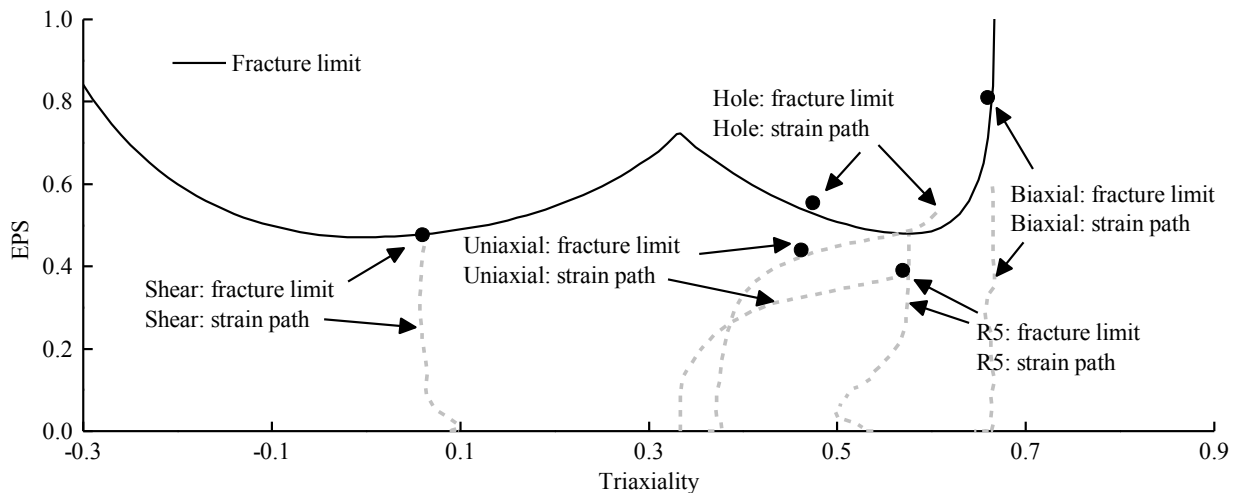
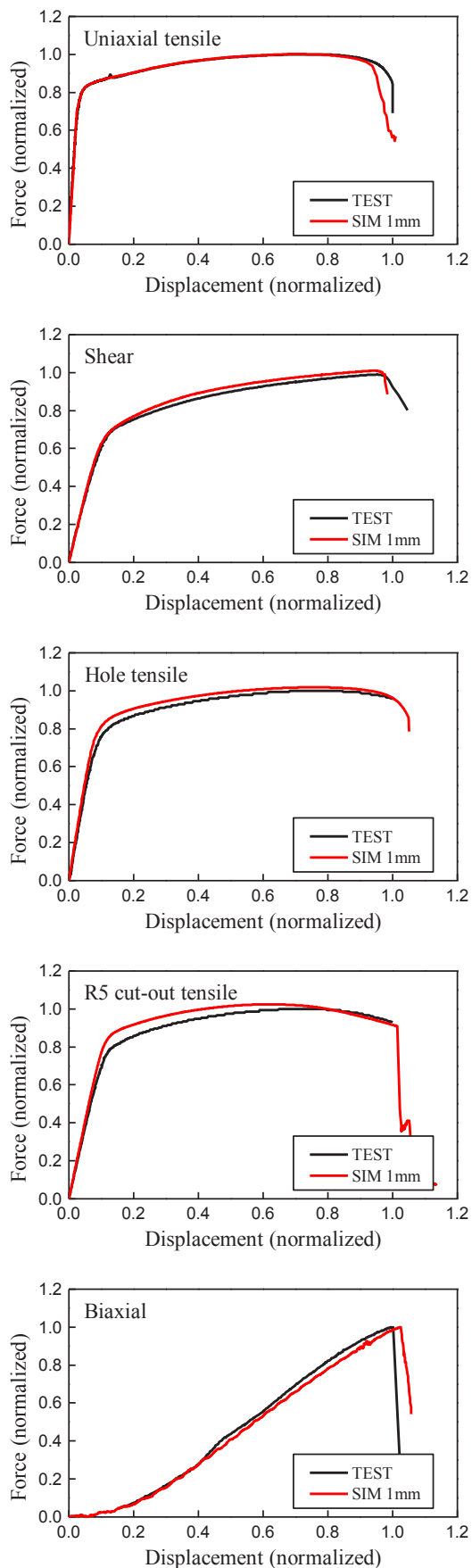


Fig. 5. Calibrated MMC fracture limit and loading path result of different test. ( $A/c_2=2.03$ ,  $n=0.18$ ,  $c_1=0.03$ ,  $c_3=0.97$ , )



**Fig. 6.** Comparison of experimental and simulation force-displacement results.

## 4 Component experiment validation

To verify the impact of stamping process on the structural performance, an open-profile bumper part made of QP1180-EL 1.2 mm in mass production was selected as the research subject. The stamping process consists of drawing, trimming and restriking operation. The three-point bending test for the stamped bumper are shown in Fig. 7, with a support span of 557 mm, a head radius of 76 mm, and a loading rate of 50 mm/minute. After the experiment, cracks occurred at the two rounded corners of the bumper's bending center, with the crack direction parallel to the length direction of the part.

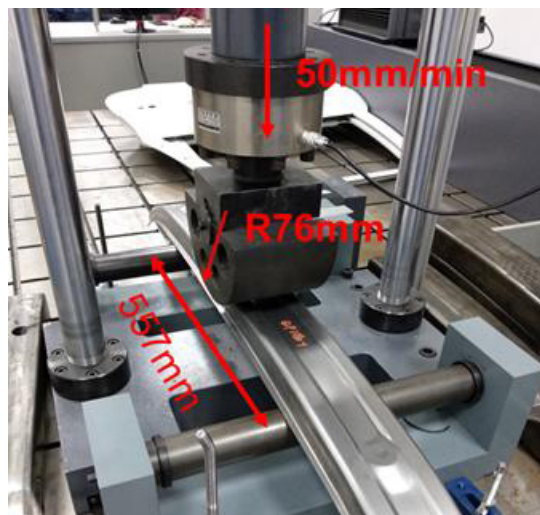


**Fig. 7.** Three-point bending test of bumper beam.

Based on actual stamping tool design and process parameters, AutoForm was used to make the full cycle simulation, with the main process defined in Fig. 8.

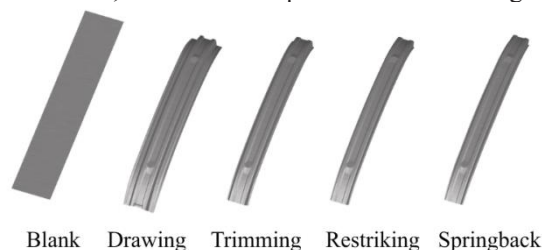


**Fig. 8.** Full cycle simulation for QP1180-EL bumper beam stamping process.

The initial damage of the parts after stamping is calculated using the simulation results of stamping process and the damage accumulation evaluation method mentioned above, and then introduced to the three-point bending simulation model, in which the bumper element size was set to 2mm and full-integrated shell element with 5 through-thickness integration points are used. Simulation was conducted using the following three conditions:

- Case 1: Excluding thinning, strain, stress, and damage during the stamping process;
- Case 2: Thinning, strain, and stress during the stamping process were included while damage history variables were excluded;
- Case 3: Thinning, strain, stress, and damage during

the stamping process were included, damage history variable of the bumper at the initial load time is shown in the Fig. 9.

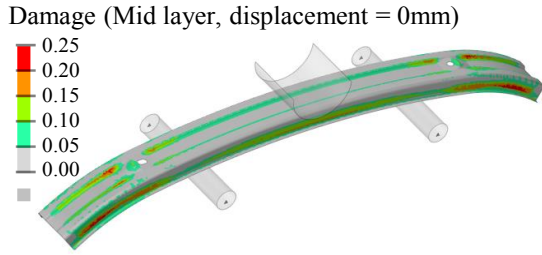


**Fig. 9.** Three-point Bending model with stamping damage.

Simulated results of local deformation under three different conditions are shown in Fig. 10 and Fig. 11. Average crack stroke of bending test was 70.6 mm, and simulated results of Case 1~3 were 88.4 mm, 79.2 mm, and 73.6 mm respectively. In addition, the average peak

force of bending test was 13.0 kN, while simulated results were 12.2 kN, 13.4 kN, and 13.4 kN respectively.

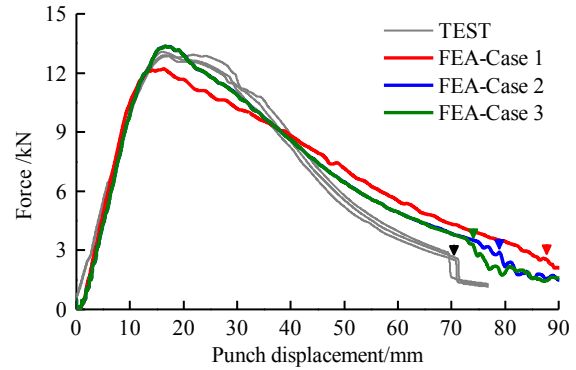


**Fig. 10.** Experiment and simulation result of three-point bending force-displacement.

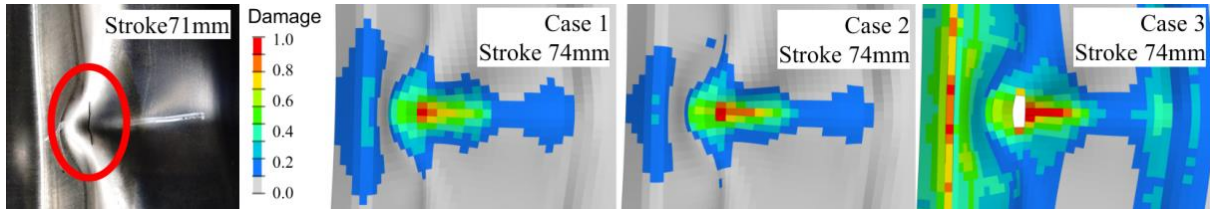


**Fig. 11.** Experiment and damage simulation result of bumper beam.

Damage accumulation process of critical element in the bending loadcase was analyzed. Simulated triaxiality and plastic strain history of the top layer (punch side) and bottom surface (support roller side) of the critical element in Fig.12 show that in the initial stage of bending process, the top surface of the critical area is subjected to tension while the lower surface is subjected to compression. After the formation of local bending corner, the top layer gradually transits from tension to compression, while the bottom layer transits from compression to tension. Damage related history variables of bottom surface of the critical element are shown in Fig. 13. The thickness reduction, strain, and initial stress caused by stamping process will affect the strain path of the local area. Ignoring the stamping forming history will result in a lower prediction of the failure risk, especially for cold stamping high-strength steel parts under large deformation conditions.

Considering the damage caused in stamping process further improve the accuracy of predicting the structural performance.

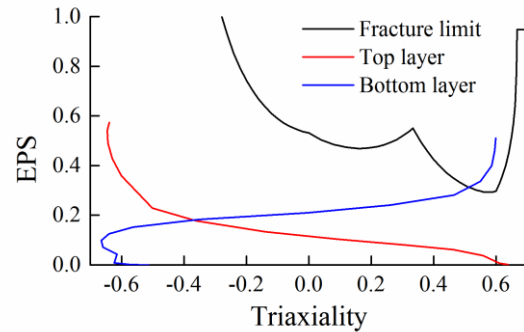


**Fig. 12.** Strain path of critical fracture element.

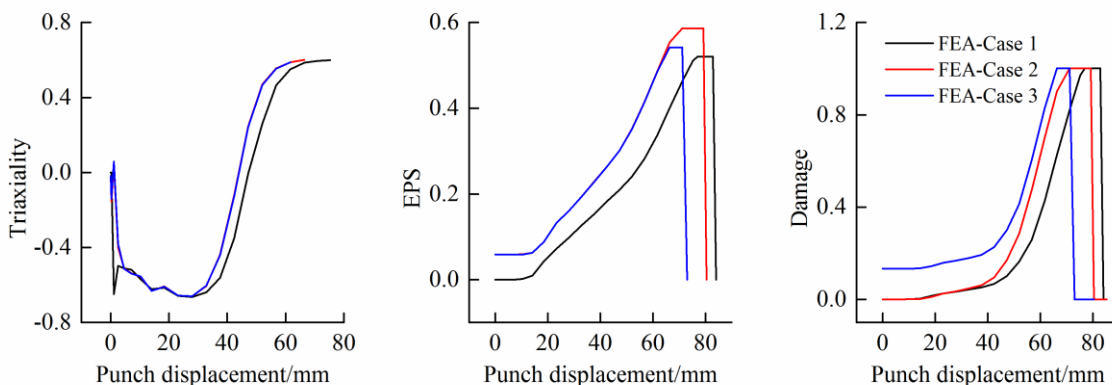


**Fig. 13.** Damage related history variables of critical fracture element.

## 5 Conclusions

Based on the assumption that the deformation process of materials during a single stamping operation follows a quasi-linear strain path, combined with the damage accumulation principle of the GISSMO damage model, a damage accumulation evaluation method for the stamping process is established, which can evaluate the damage after the stamping process.

GISSMO model with MMC fracture criterion was used to characterize the failure behavior of QP1180-EL steel. The simulated peak force and fracture displacement under the five loading conditions were consistent with the experimental results.

Three-point bending test of an open-profile stamped bumper was used to study the influence of stamping history on the structure performance of the part. Introducing stamping history, especially forming damage can improve the prediction accuracy of structural performance for ultra-high strength steel stamped parts.

## References

1. H. Yu, Z. Sun, J. Tongji Univ. Nat. Sci, **8**, 1198 (2011)
2. W. Wang, X. Sun, X. Wei, Int. J. Crashworthiness, **1**, 9 (2016)
3. J. Niu, P. Zhu, Shock VIB, **23**, 44 (2012)
4. E. Doruk, STEEL COMPOS STRUCT, **24**, 351 (2017)
5. J. Chen, C. Lian, J. Lin, IOP Conf Mat Sci & Eng., **668**, (2019)
6. F. Neukamm, M. Feucht, A. Haufe, 7th European LS-DYNA Conference (2009)
7. F. Neukamm, M. Feucht, A. Haufe, 10th International LS-DYNA Users Conference (2008)
8. F. Andrade, M. Feucht, A. Haufe, F. Neukamm, Int J Frac, **200**, (2016)
9. LSTC, LS-DYNA Keyword User's Manual – Volume II: Material Models, Livermore (2016)
10. Y. Bai, T. Wierzbicki, Int J Plast **24**, 1071 (2008)